NMR investigation of the low-temperature dynamics of solid ^{4}He doped with ^{3}He impurities

S. S. Kim,[1,*] C. Huan,[1,†] L. Yin,[1] J. S. Xia,[1] D. Candela,[2] and N. S. Sullivan[1,‡]

[1]*Department of Physics & National High Magnetic Field Laboratory, University of Florida, Gainesville, Florida 32611, USA*

[2]*Department of Physics, University of Massachusetts, Amherst, Massachusetts 01003, USA*

(Received 6 March 2013; revised manuscript received 24 May 2013; published 13 June 2013)

The lattice dynamics of solid ^{4}He has been explored using pulsed NMR methods to study the motion of ^{3}He impurities in the temperature range (0.05–0.20 K) where experiments have revealed anomalies attributed to superflow or unexpected viscoelastic properties of the solid ^{4}He lattice. We report the results of measurements of the nuclear spin-lattice and spin-spin relaxation times that measure the fluctuation spectrum at high and low frequencies, respectively, of the ^{3}He motion that results from quantum tunneling in the ^{4}He matrix. The measurements were made for ^{3}He concentrations $16 < x_3 < 2000$ ppm. For ^{3}He concentrations $x_3 = 16$ and 24 ppm, large changes are observed for both the spin-lattice relaxation time T_1 and the spin-spin relaxation time T_2 at temperatures close to those for which the anomalies are observed in measurements of torsional oscillator responses and the shear modulus. These changes in the NMR relaxation rates were not observed for higher ^{3}He concentrations.

DOI: 10.1103/PhysRevB.87.224303 PACS number(s): 67.80.bd, 67.30.hm, 76.60.−k

I. INTRODUCTION

The observation of distinctive anomalies in the frequency and dissipation of torsional oscillators (TOs) containing solid ^{4}He, often referred to as nonclassical rotational inertia fractions (NCRIFs), by Kim and Chan[1,2] has stimulated considerable activity. This is because the NCRIFs could be the signature of a supersolid state as outlined by Leggett[3] and predicted by Andreev and Lifshitz several years ago.[4] A large number of independent experiments[5–9] have shown that the NCRIF magnitude and temperature dependence are strongly dependent on defects such as ^{3}He impurities[10,11] and the quality of the crystals, and can be made very small by very careful annealing.[2] The observation of NCRIFs was preceded by reports of a striking anomaly in the measurement of sound attenuation in solid ^{4}He by Goodkind and colleagues who had compared their observations to that predicted for a true phase transition of a fraction of the solid to a supersolid state.[12,13] Additional support for the interpretation of the NCRIF anomalies in terms of a true thermodynamic phase change to a new state of matter was provided by the observation of a small but distinct contribution to the heat capacity of the solid at the same temperatures as those reported for the onset of the NCRIFs.[14]

A straightforward interpretation in terms of a transition of part of the solid to a coherent superfluid component has, however, been hampered by a number of puzzling observations. These include the lack of evidence for a critical exponent, an apparent very low critical velocity,[6] the absence of experimental evidence for fourth sound modes,[15,16] and the null results of attempts to observe pressure-induced superflow though small restrictions,[17] although mass transport has been observed with the use of porous vycor glass conduits used to allow mass flow to the solid via superfluid in the pores.[18,19] In addition, measurements of the shear modulus of solid ^{4}He by Beamish and colleagues[20,21] have revealed a prominent frequency dependent change in the elastic shear modulus with an enhanced dissipation peak having a temperature dependence comparable to that observed for the NCRIF. These results suggest that the torsional oscillator anomalies may result from unusual elastic[22] or viscoelastic[23] properties of the solid ^{4}He rather than superfluidity. Other interpretations attribute the anomalies to macroscopic superflow mediated by defects or dislocation networks[24] or in terms of a vortex model[25] for which the high temperature tail of the NCRIF is associated with the finite response time of vortices to the oscillating flow fields in the TOs. Another set of researchers suggest that the superfluidity arises from nonequilibrium behavior leading to superflow along defects or the formation of a quantum "superglass" around extended defects[26] with ultraslow relaxation dynamics reminiscent of glass dynamics.[27]

The need for any interpretation to account for both sample dependent coherent decoupled flow and changes in the lattice elastic properties was confirmed strikingly by Kim *et al.*[28] who observed that the TO response could be changed significantly by rotating the cryostat, with the resonant frequency changing with speed, but that at the same time, the TO mode that showed significant drive dependence was not susceptible to changes in the elastic modulus of the lattice.[28]

Further recent studies have confirmed that the dynamics of the ^{4}He lattice plays an important role in the low temperature bulk properties of solid ^{4}He, and rather than observing a phase transition to a supersolid state, one may be observing a complex thermally excited dynamical response.

These studies include the analyses of Maris[29] who showed that in almost all TO cell designs there was a significant previously neglected contribution to the oscillator frequency response from helium elasticity that could mimic the behavior expected for a supersolid component. In addition, Beamish *et al.*[30] showed that the frequency shift in many TOs could attributed to a "giant plasticity" of the helium in the hollow torsion rod of the device. They also found that the dislocation lengths were much larger and the dislocation networks much less connected than those needed to explain the TO effects in terms of superfluidity in a dislocation network. Finally, a new experiment by Chan *et al.*[31] using a TO design completely free from any bulk solid shear modulus stiffening effect showed no measurable anomalous TO effect attributable to a nonclassical rotational inertia.

 ©2013 American Physical Society

It is clear from all the studies, particularly the most recent, that it is important to study and understand the microscopic dynamics of solid ^{4}He using different techniques and especially noninvasive techniques since all previous studies have involved the application of macroscopic external mechanical stimuli. Measurements of the quantum tunneling of the ^{3}He atoms in the solid provide a unique means of probing microscopic lattice properties because the ^{3}He-^{4}He exchange rates depend exponentially on the lattice separation and on the magnitude and dynamics of the crystal field deformation that surround impurities.[32,33] The characteristic NMR relaxation rates are determined by the modulation of the nuclear dipole-dipole interactions by the tunneling motion and the scattering of the diffusing atoms by the crystal deformation field around the ^{3}He impurities and other lattice defects.[33,34] The NMR relaxation rates are therefore very sensitive to the local elastic properties of solid ^{4}He and to any changes in the crystal ground state that would modify the tunneling rate. We have therefore carried out systematic measurements of the nuclear spin relaxation rates of ^{3}He impurities in solid ^{4}He for a wide range of concentrations with an emphasis on low concentrations $x_3 < 30$ ppm for which one expects well characterized NCRIFs from previous studies and yet sufficient to obtain good signal to noise ratios for NMR measurements. Also for these concentrations, the amount of the ^{3}He localized on dislocations estimated from the expected density of dislocations for well-annealed samples[35] is expected to be a small fraction of the total, less than 1 ppm, so that one can be sure that the experiments probe the motion of the ^{3}He atoms through bulk solid ^{4}He. Preliminary results of these NMR studies have been reported elsewhere.[36,37]

II. EXPERIMENTAL ARRANGEMENT

The NMR cell was designed as a nested cross-coil arrangement with receiving and transmitting coils orthogonal to each other and the applied magnetic field (see Fig. 1). The inner coil is a cylindrical receiving coil wound around a polycarbonate sample cell which contained an *in situ* Straty-Adams pressure gauge. The outer coil is a thermally isolated orthogonal transmitting coil for the rf pulses that slide onto the receiving coil. This nested arrangement[38] provides (i) minimization of the unwanted pick-up of the transmitter pulse by the receiving coil, and (ii) adequate thermal isolation from the heat generated in the transmitting coil that is heat sunk to the still of the dilution refrigerator. Thermalization of the sample was assured by thermal contact with a silver post extending from the dilution refrigerator and the temperature was measured using a Cernox resistance thermometer calibrated against a ^{3}He melting curve thermometer. The sample gas was admitted via a capillary sealed with epoxy (Stycast 2850 GT) at the opposite end of the cell. The sample cell could withstand pressures up to 100 bars and remain superfluid leak-tight.

Samples were grown by the blocked capillary method. Gas samples of predetermined ^{3}He fraction were prepared at room temperature by mixing pure (99.99%) ^{3}He and ^{4}He, compressing the gas mixture to about 50 bars, and filling the sample cell with the gas mixture to a pressure of 46 bars, after which the cell was cooled to 1.2 K. When the temperature is cooled to the melting curve, the helium pressure follows the melting curve while the mixture solidifies, after which the

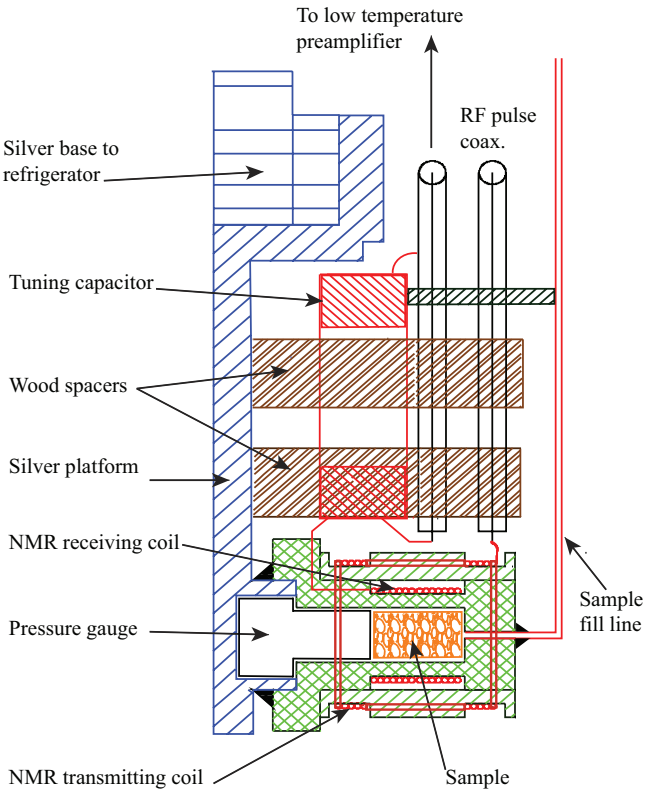

FIG. 1. (Color online) Schematic representation of the low temperature NMR cell. The sample in this NMR cell is cylindrical, 5.0 mm diameter and 7.5 mm long. The preamplifier and tuning capacitor are located on a 1 K cold plate located a distance of 1.2 m from the sample cell. The rf transmitting and receiving coils are simplified in this figure.

pressure measured by the gauge in the cell remains constant indicating that the sample is solid. The samples were prepared to all have the same final pressure of 27.75 ± 0.05 bars at 1.2 K. The molar volume of the samples were determined to be $V_m = 20.85 \pm 0.05$ cm^3 from the PVT data of Grilly and Mills[39] and the formula derived by Mullin.[40] Finally the samples were annealed for 24 h just below the melting point except for one case for which a minimum annealing of 0.5 h was carried out to determine the effect of the crystal quality on the nuclear spin relaxation times.

The measurements of the nuclear spin-spin and spin-lattice relaxation times were carried out using a superheterodyne pulsed NMR spectrometer operating at a Larmor frequency of 2.05 MHz. At this frequency the calculated relaxation times due to exchange motion were of the order of 10^4 s at ^{3}He concentrations $x_3 = 20$ ppm, extrapolating from previous measurements.[41–44] The longitudinal relaxation time is expected to increase rapidly with frequency,[41] making studies at higher Larmor frequencies extremely difficult.

The signal/noise ratio for samples with $x_3 \approx 20$ ppm is very weak ($<10^{-2}$) for a 10 kHz bandwidth employing a standard geometry with resonant NMR circuit connected directly to a room temperature amplifier. In order to enhance the signal/noise we developed a preamplifier that could be operated at low temperatures in the applied magnetic field.[38] The device used a pseudomorphic high electron mobility field

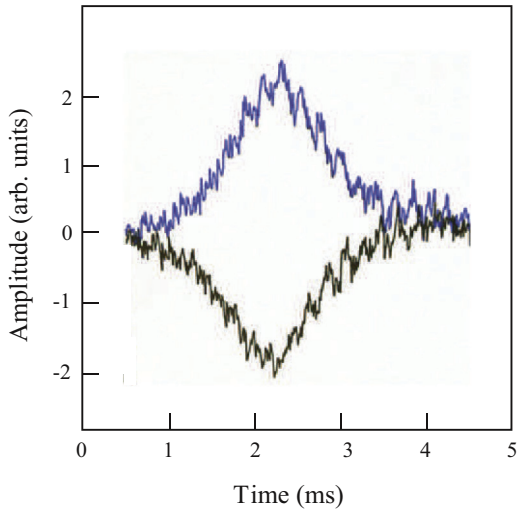

FIG. 2. (Color online) Example of NMR Hahn echo for a sample of 500 ppm ^{3}He in solid ^{4}He at $T = 0.4$ K, showing the in-phase and out-of-phase components.

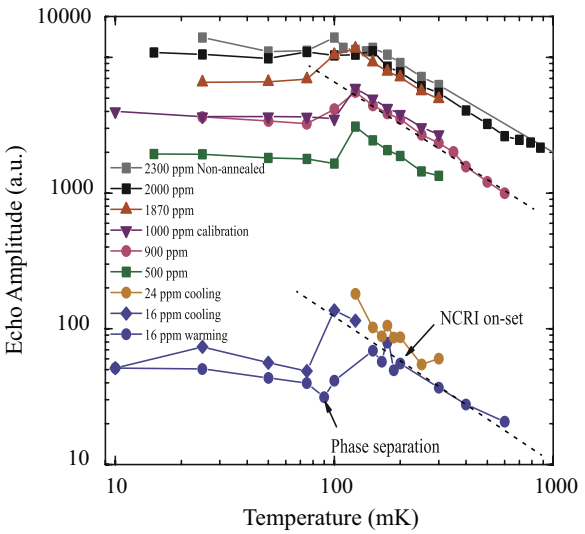

FIG. 3. (Color online) Observed temperature dependence of NMR echo amplitudes for several different samples measured for the same spectrometer pulse and gain settings. The broken lines represents the Curie-law behavior.

effect transistor with adjustable bias so that the output could be matched to a 50 ohm cable. The total power dissipation was 0.5 mW and to attain the lowest sample temperatures the amplifier was separated from the sample cell by a 75 cm length of cable and anchored to a 1 K thermal plate. A typical NMR echo recorded using a 90_x–180_x rf pulse sequence for a 500 ppm ^{3}He sample is shown in Fig. 2 after signal averaging for 10 pulse sequences using a 17 kHz bandwidth. As it is necessary to wait several times T_1 between pulse sequences, up to 15 h were required to obtain each data point at the lowest temperatures. Therefore the total number of data points is modest, but sufficient we believe to reveal and confirm relevant features in the temperature dependence of the relaxation times.

One of the most important properties of the sample that must be determined is the exact ^{3}He concentration, because for the long capillary line used (1.2 m below the 1 K plate) an appreciable fraction of the ^{3}He atoms can plate out on the capillary walls and lead to changes in the ^{3}He concentration of the solid sample compared to that of the original gas concentration. Fortunately, the NMR signal itself allows one to obtain an accurate calibration by measuring the NMR echo amplitude for fixed spectrometer gain at intermediate temperatures and comparing it to a relatively high concentration sample (2000 ppm) for which any fractional change would be small. In Fig. 3 we show the temperature dependence of NMR echo amplitudes for several different samples. All the samples show the characteristic Curie law behavior until reaching temperatures of the order of 0.1 K where phase separation occurs. At these low temperatures the ^{3}He forms Fermi liquid droplets with temperature independent NMR amplitudes and with different relaxation times. Using this procedure one can measure the ^{3}He concentration to approximately 5% accuracy. For example, for a sample prepared from a nominally 30 ppm gas mixture, the final solid ^{3}He fraction was measured to be 24 ppm. Note that a small deviation was observed in the amplitude of the echo signal for the 16 ppm sample at $T = 175$ mK and this is attributed to the sudden and unexpected sharp increase in T_1 at that temperature. Waiting times between measurements were set at 5 times T_1 to provide 5% accuracy in amplitude measurements but at 175 mK this drops to 2.5 times T_1 and a small decrease in observed amplitude results.

III. EXPERIMENTAL RESULTS

Figure 4 shows the observed temperature dependence of the nuclear spin-lattice relaxation time (T_1) and the spin-spin relaxation time (T_2) for a sample with $x_3 = 16$ ppm and the comparison with the results for a sample with $x_3 = 500$ ppm. The temperature independent tunneling induced relaxation occurs for $0.2 < T < 0.55$ K and a small upturn in T_1 is observed for $T > 0.55$ K with a corresponding downturn in T_2. This high temperature behavior is attributed to the onset of the effect of thermally activated vacancies. The most interesting features are the sharp peak in T_1 at $T = 175$ mK and a less well-defined minimum in T_2 at the same temperature

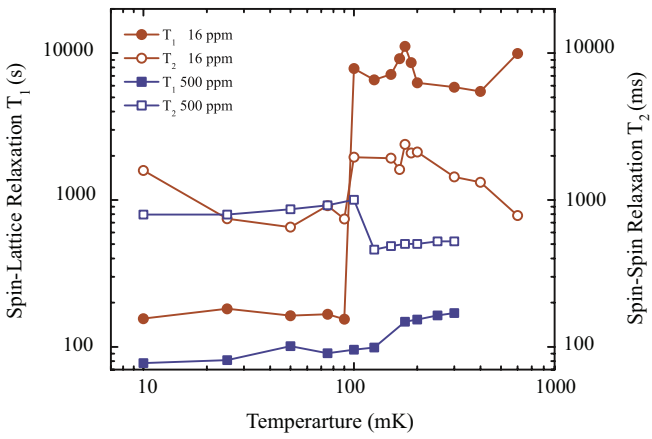

FIG. 4. (Color online) Observed temperature dependence of the spin-lattice and spin-spin relaxation time for two samples (i) $x_3 = 16$ ppm, and (ii) $x_3 = 500$ ppm.

for the sample with $x_3 = 16$ ppm. The same behavior as a function of temperature is observed for a sample with $x_3 = 24$ ppm prepared with a considerably reduced annealing time.[37] The sharp changes in T_1 and T_2 are not observed for samples with concentrations $x_3 > 200$ ppm. These features near 175 mK are unexpected in the traditional interpretations of the relaxation of dilute ^{3}He in solid ^{4}He that attribute the relaxation to a temperature independent quantum tunneling J_{34} of the ^{3}He atoms through the ^{4}He lattice. The temperatures at which these sharp features for T_1 and T_2 occur coincide with the temperatures for which anomalies are observed for measurements of the rotational inertia[1,2] and shear modulus experiments.[21,45] On cooling below 175 mK, a precipitous drop in the value of T_1 is observed at $T = 95$ mK, which is the temperature associated with the phase separation of the solid mixture into ^{3}He rich droplets in otherwise pure solid ^{4}He. This interpretation is confirmed by the observed change in the NMR amplitude below the phase separation temperature as shown in Fig. 3 and by the significant hysteresis on cycling through the phase separation temperature.[37]

IV. DISCUSSION

The nuclear spin-lattice and spin-spin relaxation times are determined by the modulation of the dipole-dipole interactions H_{dd} between the ^{3}He atoms. The modulation arises from the motion of the atoms either due to ^{3}He-^{4}He quantum tunneling (particle exchange) or ^{3}He-vacancy exchange for solid ^{3}He-^{4}He mixtures. The latter is only observed above approximately 0.5 K because the number of thermally activated vacancies is otherwise extremely small. The relaxation rates are calculated in terms of the spectral densities (or Fourier transforms) of the time dependent autocorrelation functions $\langle H_{dd}(t)H_{dd}(0)\rangle$ with the component of the spectral densities at the Larmor frequency and twice the Larmor frequency determining the spin-lattice relaxation and the component at zero frequency determining the spin-spin relaxation for the cases where the Larmor frequency is greater than the modulation frequency. This view is valid only when the tunneling excitations (atom or vacancy exchange) are in good thermal contact with the fundamental lattice excitations (phonons). If that is not the case, a phonon bottleneck for the relaxation can be observed with a remarkable T^{-6} dependence at very low temperatures. For a general treatment of the well-established relaxation mechanisms in solid and liquid He, the reader is referred to Abragam and Goldman.[46] The motion of the ^{3}He atoms is not that of a bare particle. Because the zero point motion of a ^{3}He atom is greater than that of a neighboring ^{4}He atom, there is an appreciable lattice deformation around a ^{3}He atom and this deformation and its motion depends on the plasticity of the lattice. If there is a change in the fundamental lattice properties this can be observed through measurements of the NMR relaxation times.

The theoretical treatments of the relaxation of dilute ^{3}He atoms in solid ^{4}He[33,34,47–50] all take into consideration the lattice deformation surrounding a ^{3}He impurity. The deformation has been described in terms of a long range anisotropic interaction between ^{3}He atoms given by

$$K(r_{ij}) = K_0(3\cos^2\theta_{ij} - 1)\left(\frac{a_0}{r_{ij}}\right)^3 \quad (1)$$

for the deformation energy at site j due to an impurity at site i, where a_0 is the lattice constant.[32,51] The ^{3}He atoms travel through the lattice and scatter from one another with a closest approach given by the distance b_c for which the kinetic energy of the tunneling particle ($\sim J_{34}$) becomes comparable to the elastic deformation energy

$$b_c = \left(\frac{J_{34}}{K_0}\right)^{1/3} a_0. \quad (2)$$

The mean separation of the ^{3}He atoms $r_m = a_0 x_3^{-1/3}$ and for $x_3 \geqslant x_{30} = \frac{J_{34}}{K_0} \sim 10^{-3}$ the ^{3}He atoms are in continuous interaction with elastic fields of one another. For $x_3 < x_{30}$, the atoms move coherently by tunneling until scattered by other ^{3}He atoms or other lattice defects. This simple estimation of the concentration x_{30} for which there is a crossover from simple coherent diffusion to the continuous interaction regime was analyzed in detail by Landesman and Winter[48] using a moment expansion for the calculation of the physical diffusion and they found a very different value with $x_{30} \sim (\frac{J_{34}}{K_0})^2 \sim 10^{-6}$. Huang *et al.*[34] re-examined this estimate using a more precise accounting of of the energetics of the scattering process and estimated $x_{30} \sim 10^{-4}$. As we will show below, the Landesman model gives a good description of the values of the spin lattice relaxation time measured by different research groups with a characteristic concentration dependence of $T_1 \propto x_3^{-2/3}$ for $x_3 > 10^{-4}$ and a very different concentration dependence below 10 ppm.

In order to understand the possible origins of the experimentally observed peak in T_1 at low temperatures, we need to examine how the tunneling motion of the ^{3}He atoms and their accompanying lattice deformations determine the nuclear spin-lattice relaxation. Landesman[33] treated the motion of the ^{3}He atoms in the presence of the deformations using a fictitious spin model. In this model a fictitious spin S_i takes the values 0 or ± 1 according to whether a site i is occupied by a ^{4}He atom or a ^{3}He atom with real nuclear spin $I_j^z = \pm 1$, respectively. The probability that a site j is occupied by a ^{3}He atom is represented by $\tau_j = (S_z^j)^2$ and the elastic deformation energy by the Hamiltonian

$$H_K = -2\hbar \sum_{jk} K_{jk}\tau_j\tau_k. \quad (3)$$

The tunneling Hamiltonian is given by

$$H_T = -2\hbar J_{34} \sum_{j,k} P_{jk}, \quad (4)$$

where $P_{jk} = \frac{1}{2}(S_j^z S_j^+ S_k^- S_k^z + S_j^z S_j^- S_k^+ S_k^z) + \text{H.c.}$ is the permutation operator for atoms at sites i and j.

The time dependence of the fictitious spin operators S_j and τ_j are given by

$$S_j^+(t) = e^{iH_K t} S_j^+ e^{-iH_K t} = S_j^+ e^{i\omega_j t}, \quad (5)$$

where $\omega_j = 2\sum_{j<k} K_{jk}\tau_k$. In this time dependence Landesman did not include a lattice relaxation term to account for relaxation of the lattice as the deformation surrounding the impurity atom moves through the lattice. Given the recent results from elastic studies of solid helium at low temperatures this could be an important effect. The relaxation times can now

be estimated by calculating the correlation functions of the nuclear dipole-dipole interactions. We consider the reduced correlation function

$$\Gamma^m_{ijkl} = \frac{4}{x_3}\langle T^m_{ij}(t) T^m_{kl}(0)^\dagger\rangle, \tag{6}$$

where the T_{ij} are the irreducible nuclear spin operators [that transform analogously to the spherical harmonics $Y^m_2(\Omega_{ij})$]. $T^m_{ij}(t) = e^{iH_M t} T^m_{ij} e^{-iH_M t}$ with $H_m = H_K + H_T$ the total Hamiltonian responsible for the motions in the lattice. For the dilute lattice the tunneling Hamiltonian does not commute with all T_{ij} and one finds that the derivative

$$\ddot{\Gamma}_{ij,ij}(t)/\Gamma(0) = -12 x_3 J_{34}^2 \sum_p F_{ip}(t)\cos[(K_{ij} - K_{jp})t]\left(\frac{a_0}{r_{ij}}\right)^6, \tag{7}$$

with $F_{ip}(t) = \prod_s \cos[\omega_s(t)]$, where $\omega_s = x_3(K_{is} - K_{ps})t$. Evaluating $F(t)$ using the statistical method of Anderson[52] yields

$$\ddot{\Gamma}(t)/\Gamma(0) = -48\Lambda' x_3 J_{34}^2 \exp[-x_3\Lambda(K_0 t)^{3/4}], \tag{8}$$

where $\Lambda' = 0.28$ and $\Lambda = 8.77$.[33,48] Integrating Eq. (8) Landesman[33] finds a correlation time τ_c given by

$$\tau_c^{-1} = B\frac{J_{34}^2}{K_0} x_3^{-1/3}, \tag{9}$$

with $B = 23$.

The correlation time $\tau_c < \omega_L^{-1}$ for all the experiments reported and we therefore find for the calculated nuclear spin-lattice relaxation time in Landesman's model

$$T_1^L = \frac{\omega_L^2}{46 M_2}\frac{1}{J_{\rm eff}} x_3^{-2/3}, \tag{10}$$

where M_2 is the second moment for pure ^{3}He and $J_{\rm eff} = J_{34}^2/K_0$. As shown in Fig. 5 this calculated value provides a good description of the observed values of T_1 in the temperature-independent "plateau" region for ^{3}He concentrations $x_3 > 100$ ppm for $\frac{J_{\rm eff}}{2\pi} = 1.2$ kHz and no other adjustable parameter. At lower concentrations a much stronger concentration dependence is observed with $T_1 \propto x_3^{-4/3}$. This behavior at low concentrations is attributed to the crossover from the continuous interaction regime to a region of coherent diffusion for which the characteristic time is determined by the time for a ^{3}He atom to travel the mean distance $r_m = x_3^{-1/3} a_0$ between ^{3}He atoms. This time is given by $\tau_{\rm coh} = r_m/v_g$, where the group velocity $v_g = a_0 z J_{34}$. The best fit to the low concentration data is given by $T^{\rm Coh}_{1(\rm Emp)} = 2.5\times 10^{-3} x_3^{-(4/3)}$ shown by the solid red line of Fig. 5, and corresponding to $J_{34}/(2\pi) = 0.83$ MHz.

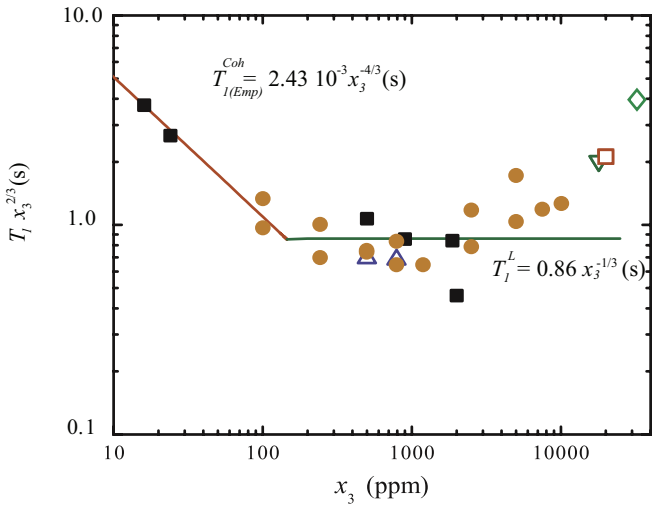

FIG. 5. (Color online) Observed ^{3}He concentration dependence of the nuclear spin-lattice relaxation time for dilute ^{3}He in solid ^{4}He. Orange circles, Schratter *et al.*,[43] up triangles, Allen *et al.*,[53] diamonds, Schuster *et al.*,[54] down triangles,[55] open squares,[44] and solid squares.[37]

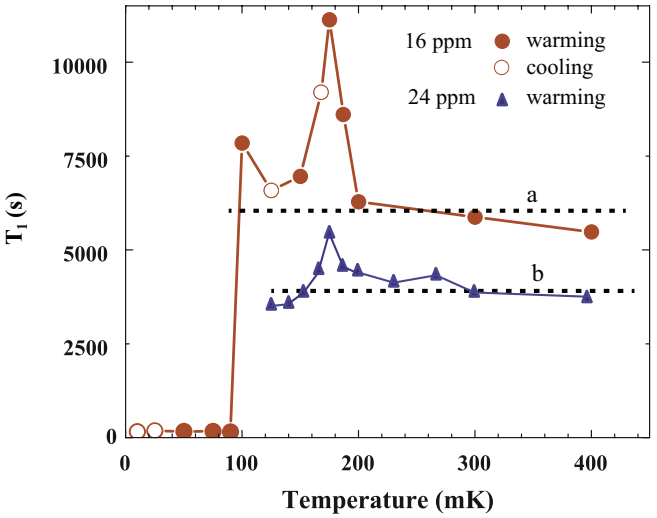

FIG. 6. (Color online) Comparison of the values of the observed nuclear spin-lattice relaxation times for $x_3 = 16$ ppm (red circles) and $x_3 = 24$ ppm (blue triangles) with the theoretical model of Landesman (broken lines a and b) for tunneling ^{3}He impurities in the ^{4}He lattice with a fixed lattice distortion. The sharp drop at 90 mK marks the well known phase separation with the formation of pure ^{3}He nanodroplets. The 24 ppm sample was never cooled below 120 mK to avoid hysteresis and memory effects associated with the phase separation.

The empirical fit to the temperature independent relaxation for $x_3 = 16$ and 24 ppm is shown by the broken lines in Fig. 6. While the fit to experimental data is good at high temperatures the anomalous relaxation observed at 175 mK is more than a factor of 2 larger than the Landesman prediction for a simple tunneling motion of the ^{3}He atoms through the lattice. The anomaly occurs well above the phase separation temperature (90 mK) and is not attributable to the phase separation which would lead to a sharp decrease in the relaxation time and not the sharp peak that was observed. This conclusion was confirmed by studying a sample with 24 ppm that was never cooled to the phase separation temperature (see Fig. 6).

It is important to note that a simple change in the elastic field interaction K associated with thermal population of excited states with different values for K_0 would not explain the observed results and would simply lead to a broad step in the value of T_1. The results therefore imply that the anomalous peak observed for T_1 results either from a change in the

dynamical properties of the lattice that occur at 175 mK or that there is a phase transition that occurs at that temperature and the peak observed in T_1 results from the fluctuations at the phase transition.

A. Effect of a transition to supersolid state on the NMR relaxation times

We now consider what would be expected if there was a simple phase transition to a state in which there was a small fraction of superfluid condensate, and then we will discuss how the effect of a dynamical relaxation of the lattice as described by Beamish and colleagues would influence the nuclear spin lattice relaxation time T_1.

If there was a sharp phase transition at a fixed temperature T_C below which a superfluid state appears, one would expect a sudden change in the spectral density at T_C that determines T_1 and T_2 because of the sharp increase in fluctuations just below T_C that would modulate the spin-spin interactions (assuming that the ^{3}He atoms are carried by the superfluid component). One of the most significant results of Chan *et al.*[2] is that the critical velocity attributed to the superfluid interpretation of the NCRIFs is very low, typically 10^{-4} m/s. The fluctuations would therefore add weight to the spectral density at low frequencies and not at high frequencies (>MHz). Because the spectral densities are determined by the fluctuations of the ^{3}He dipole-dipole interactions (and no other magnetic interactions are present) they are normalized and thus the increase in spectral weight at low frequencies would result in a decrease in the spectral weight at high frequencies with an increase in T_1 and a concommittant decrease in T_2.

If we designate the component of the spectral density due to ^{3}He particle exchange as $J_E(\omega)$ and the component due to a possible superfluid component as $J_S(\omega)$, we have

$$\int \frac{1}{T_1} d\omega = \int [J_E(\omega) + J_S(\omega)] d\omega = \pi M_2, \qquad (11)$$

where M_2 is the NMR second moment. For liquid ^{4}He the coherence length scales as $\xi = a_0(T_C - T)^{-2/3}$, where T_C is the critical temperature, and because of the very low critical velocities (inferred from torsional oscillator measurements), we anticipate a characteristic relaxation time that behaves as $\tau_s = \tau_{so}(T_C - T)^{-2/3}$ for $T < T_C$, using $\tau_{so} \cong r_m/v_c$, where $r_m = x^{-1/3}a_0$ is the mean separation between atoms, a_0 is the lattice spacing, and v_c is the critical velocity. If the supersolid component component has weight $\alpha(T)$ then the exchange component must have weight $1 - \alpha(T)$ so that the sum rule $\int \frac{1}{T_1} = \pi M_2$ is obeyed. Thus the observed relaxation rate will be given by

$$\frac{1}{T_{1\mathrm{Obs}}} = \alpha(T) J_S(\omega_L) + [1 - \alpha(T)] J_E(\omega_L), \qquad (12)$$

where $J_S(\omega_L)$ is negligible. If T_{1E} is the calculated value of T_1 for exchange motion only, we find

$$\frac{T_{1\mathrm{Obs}}}{T_{1E}} = \frac{1}{[1 - \alpha(T)]}, \qquad (13)$$

where for a supersolid fraction we take $\alpha(T) = a_1 \frac{T_0}{|T - T_C)|^{2/3}}$ for $T < T_C$ and $\alpha(T) = 0$ for $T > T_C$. a_1 is an adjustable parameter related to the "supersolid" density which is of the order of 0.01 but sample dependent.

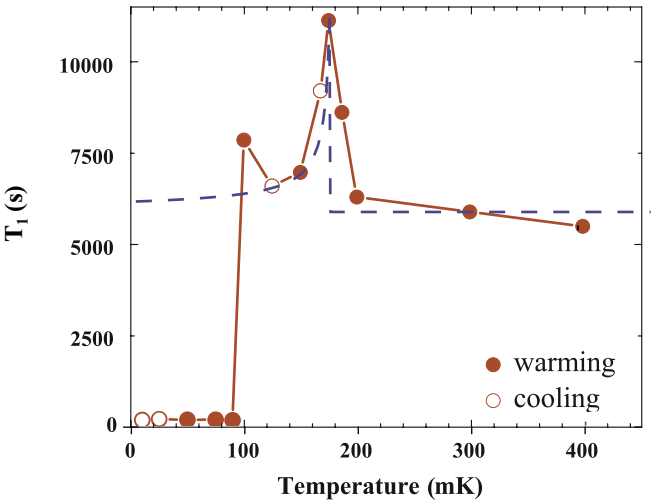

FIG. 7. (Color online) Comparison of the observed temperature dependence of the nuclear spin-lattice relaxation time T_1 with the dependence expected for a true phase transition at $T = 175$ mK for a sample with $x_3 = 16$ ppm as described in the text.

An example of a fit using the above expression for $T_{1\mathrm{Obs}}$ is shown by the broken line in Fig. 7 for $T_C = 175$ mK and $a_1 = 0.01$ with no other adjustable parameter. In reality we would expect to have a small Gaussian spread (of about 7 mK) in the critical temperature because of the inhomogeneities and it would not be difficult to obtain a good fit to T_1 for reasonable numbers but no other experiment points to a sharp transition (except for the onset of NCRIFs in very pure samples), e.g., no sharp peak in the heat capacity is reported. A more stringent test of this interpretation is provided by examining the results for the T_2 measurements for the same sample. The same argument as used for evaluating T_1 needs to be followed for T_2 but this time we need to know the values for τ_{s0} and the exchange time τ_E.

First we consider the theoretical predictions for T_2 for small x_3. The values of the correlation time calculated by Landesman [Eq. (10)] that give a good fit to the T_1 data do not lead to values of T_2 that are in agreement with the experimental data. This discrepancy has been reviewed by Kim *et al.*[56] who showed that the detailed spectral density at low frequencies cannot be described by a single Lorentzian spectral density. A better approach to evaluating T_2 was given by Huang *et al.*[34] who calculated the scattering of tunneling ^{3}He impurities in the elastic crystal fields using detailed energy conservation and found $T_2^H = 1.69 \times 10^{-4} x_3$ s for $x_3 > 100$ ppm. This result is compared with the experimental data and Landesman's theory in Fig. 8. For very dilute concentrations, $x_3 < 100$ ppm, the model of coherent diffusion as discussed above gives $T_2^{\mathrm{Coh}} = 1.68$ s.

For these dilute samples the tunneling motion of the ^{3}He impurities would lead to a temperature independent relaxation, but once again we observed strong deviations from temperature independence below 175 mK. However, unlike the T_1 results which show a clean peak, there is considerable scatter in the T_2 data and the dependence observed is that of a small peak followed by a strong dip, and then at even lower

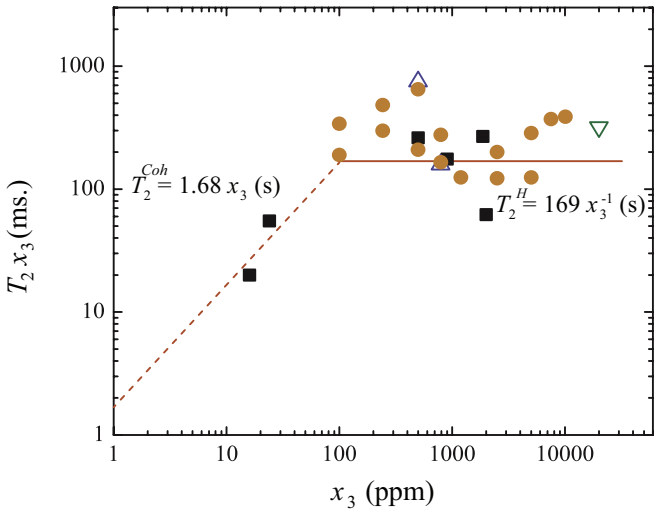

FIG. 8. (Color online) Observed ^{3}He concentration dependence of the nuclear spin-spin relaxation time for dilute ^{3}He in solid ^{4}He for several concentrations reported by different authors. The solid lines T_2^L and T_2^H are the predictions of the theories of Landesman[33] and Huang *et al.*,[34] respectively. $T_2^{\rm Coh}$ is the value of T_2 for coherent diffusion where the mean separation is greater than the scattering length. See legend of Fig. 6 for definition of symbols.

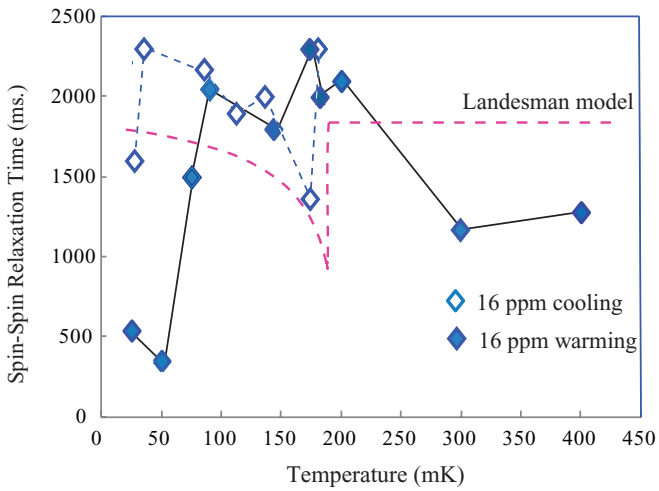

FIG. 9. (Color online) Comparison of the observed temperature dependence of the nuclear spin-spin relaxation time T_2 for a sample with $x_3 = 16$ ppm with the dependence expected for a true phase transition at $T = 175$ mK (broken purple line) as described in the text with the high temperature limit given by Landesman's model.

temperature there is an order of magnitude drop at the phase separation temperature where Fermi liquid droplets form. We now calculate what would be expected for a simple superfluid phase transition. In terms of the spectral densities (at zero frequency) for the superfluid and normal components we have

$$\frac{1}{T_{2\rm Obs}} = \alpha(T) J_S(0) + [1-\alpha(T)] J_E(0), \tag{14}$$

while the fixed temperature independent tunneling term is

$$\frac{1}{T_{2E}} = J_E(0). \tag{15}$$

We therefore find

$$\frac{T_{2\rm Obs}}{T_{2E}} = \frac{1}{b\alpha(T) + [1-\alpha(T)]}, \tag{16}$$

where $b = J_S(0)/J_E(0) = \tau_{S0}/\tau_E > 1$ and τ_E is the characteristic tunneling time in the normal solid. Because of the large value of b, the result for $T_{2\rm Obs}$ does not look like the inverted image of T_1 (as one would naively expect) but is much wider. An example of an attempted fit for the adjustable parameters $b = 4$ and $a_1 = 0.01$ is shown in comparison with experimental values of T_2 in Fig. 9. Even allowing for the scatter of the data, this approach does not provide a good description of the temperature dependence of T_2. We should note that if the system is very inhomogeneous with different parts of the sample having different values of b and a_1 one would expect a lumpy spectral density at low frequencies and a corresponding scatter in the results for T_2, but since T_1 measures the spectral weight at MHz frequencies, one could still observe a sharp peak for T_1 because it is the integrated weights of the low frequency components of the spectral densities that must be subtracted from the high frequency spectral density. In this sense the T_1 measurements are a much cleaner test for the existence of a phase transition that the T_2 measurements.

B. Effect of lattice dynamics on the NMR relaxation rates

An alternative approach to interpreting the NMR relaxation rates is to assume that as a result of the tunneling of the ^{3}He atoms there is an internal stress on the ^{4}He lattice as the distortion around the ^{3}He impurity moves with or attempts to move with the impurity as it tunnels from site to site. The mean frequency of this motion is $\omega_x = x^{4/3} K_0 \approx 3.5 \times 10^3$ Hz. We can surmise that the relaxation of the lattice due to this time dependent disturbance is long and adds a bottleneck for energy exchange between the tunneling excitations and the thermal bath of phonons. The correlation function for the lattice operators $\tau(T)$ of Eq. (3) can be written as

$$\langle \tau(t)\tau(0)\rangle = \langle \tau(0)^2\rangle_R \exp\left(-i\omega_x + \tau_S^{-1}\right)t, \tag{17}$$

where $\langle\cdots\rangle_R$ represents an average over lattice coordinates, τ_S is the lattice averaged relaxation time which we assume corresponds to the Debye relaxation $\tau_S = \tau_0 \exp(E_0/T)$ used to interpret the results of the shear modulus measurements.[20–22] Integrating Eq. (17) we find for the additional lattice relaxation time

$$\tau_x(T) = r_1 \frac{\tau_0 e^{E_0/T}}{1 + (\omega_x \tau_0 e^{E_0/T})^2} = \frac{r_1}{\omega_x}\frac{u}{1+u^2}, \tag{18}$$

where $u = \omega_x \tau_0 e^{(E_0/T)}$. τ_0 and E_0 are adjustable parameters that we expect to be comparable to the values determined from the shear modulus experiments.[22,45] The magnitude of r_1 can be estimated crudely from the relaxation rate $R = \frac{\omega_x}{r_1}$ using the golden rule with $R = \frac{4\pi}{\hbar}\sum_E |\langle E_1|K|E_2\rangle|^2 \rho(E)\delta(E_1 - E_2 - \hbar\omega_x)$ for an attempt frequency ω_x. K is the lattice distortion and the density of states $\rho(E) \sim E^2/E_D^3$, where E_D is the Debye energy. We find $R \sim 1.2 \times 10^{-4}$ s^{-1}. In Fig. 10 we show the fit to the relaxation times T_1, using $T_{1\rm Obs} = T_{1E} + \tau_x(T)$

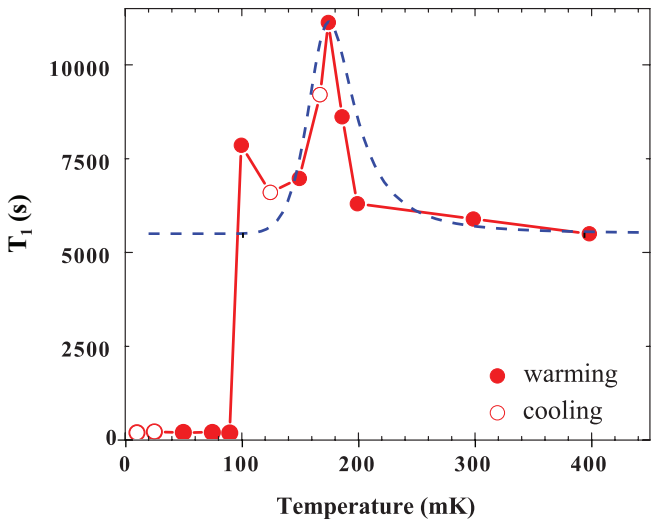

FIG. 10. (Color online) Comparison of the observed temperature dependence of the nuclear spin-lattice relaxation time T_1 (for a sample with $x_3 = 16$ ppm) with the dependence calculated for lattice relaxation due to the motion of the distortion of the lattice around impurities, using parameters inferred from the measurements of the shear modulus.

for $\tau_0 = 8.3 \times 10^{-9}$ s and $E_0 = 1.8$ K. These values are to be compared with those inferred from the shear modulus experiments,[20–22] $\tau_0 = 2.3 \times 10^{-9}$ s and $E_0 = 0.77$ K.[20] The larger value of E_0 may result from the presence of larger ^{3}He concentrations in the NMR experiments compared to the shear modulus experiments. Although the values of τ_0 and E_0 are different from those deduced by Beamish *et al.*,[21,22] the fit is quite good given the approximations that have been made. It is important to note that the observed relaxation is the sum $T_{1(\mathrm{Emp})}^{\mathrm{Coh}} + \tau_X(T)$ of the temperature independent coherent relaxation and the lattice relaxation $\tau_X(T)$ which act in series. The longest time of the two components determines the observed relaxation and only the peak of the Lorentzian form of $\tau_X(T)$ is seen at low temperatures

This interpretation of the results is consistent with the observations of Sasaki *et al.*[57,58] who followed the temperature dependence of the NMR signals of 10 ppm ^{3}He in solid ^{4}He for densities such that the phase separation forms solid clusters of ^{3}He. While they were able to observe the solid clusters they were not able to detect the signal from isolated ^{3}He atoms above the phase transition at low temperatures, and they attributed this to a long spin-lattice relaxation time that lead to saturation and signal loss at the temperatures of interest for exploring the anomalies of the ^{4}He lattice.

C. Effect of dislocations on relaxation times

The most significant effect of the presence of dislocations on the NMR studies is that the ^{3}He atoms will pin the dislocation lines leaving some of the ^{3}He atoms located on the dislocation lines and the lines themselves essentially immobile at low temperatures. The number of ^{3}He atoms that are expected to be affected by this is very small. The localization of the ^{3}He atoms would lead to three distinct components of the NMR signals and their relaxation: (i) the contribution from atoms fixed on the dislocation lines, (ii) the interactions between fixed localized ^{3}He atoms with those tunneling freely in the solid, and (iii) the interactions between pairs where both are free to move in the lattice. The latter has been the focus of the discussions above. For those atoms that are essentially fixed the line shapes would be very broad leading to short values of T_2 and very long values for T_1. The echoes would have more than one contribution and if the numbers of fixed atoms were significant the echo would have a central peak, corresponding to the spin-spin interactions between immobile atoms. We have not observed such a peak or a deviation from a single exponential decay for the dilute samples down to the lowest temperatures studied.

This result is not surprising when one considers the number of dislocations present even in crystals of average quality. Paalanen *et al.*[59] and Iwasa *et al.*[35,60] show that the dislocation density Λ and the dislocation network length L_N are related by $\Lambda L_N^2 = 0.2$ and $\Lambda \cong 10^6$ cm^{-2} with $L_N \sim$ (3–6) $\times 10^{-4}$ cm $\sim 10^4 a_0$. The concentration of ^{3} He atoms that would saturate the dislocation network is therefore estimated as $x_{3s} \sim (\frac{a_0}{L_N})^2 \sim 10^{-8}$. The dislocation density would need to be much larger than that expected for even average quality crystals[35,60] if the pinned ^{3}He atoms were to be observable. Recent experiments by Haziot *et al.*[61] imply that for crystals grown by the blocked capillary method ΛL_N^2 is about 100 times larger than the estimate given above, but that the dislocation density Λ is close to the estimate above. These new data do not change our conclusions.

In addition to dislocation lines, Balibar has pointed out[62] that grain boundaries are also likely to bind ^{3}He impurities—possibly affecting NMR relaxation times in a temperature-dependent manner. A key parameter determining the importance of grain-boundary binding is the typical grain size L_G. We have no direct information on L_G for our blocked-capillary samples, although, for example, $L_G \approx 0.5$ mm was observed by Franck *et al.*[63] in annealed helium films.

The grain size L_G controls any possible effect of grain-boundary binding on the NMR response in two distinct ways: (a) The maximum concentration of ^{3}He that can be bound at grain boundaries is of order a_0/L_G, assuming full monolayer coverage with bound ^{3}He, and (b) the time scale for ^{3}He atoms to freely diffuse on and off grain boundaries is of order L_G^2/D, where D is the diffusion coefficient. For $L_G = 0.5$ mm we calculate $a_0/L_G = 0.7$ ppm, much less than the ^{3}He concentrations used in the present experiments. For a diffusion constant $D = 3 \times 10^{-6}$ cm^2/s[53] we find $L_G^2/D \approx 10^3$ s, much shorter than the relaxation times T_1 that we observe. The latter implies that the collisions between the ^{3}He impurities in the bulk sample dominates the relaxation process. Therefore, it appears that the grain size in our samples would need to be much smaller than was observed in films in Ref. 60 for the binding of ^{3}He atoms at grain boundaries to be the cause of the T_1 anomalies we observe.

D. NMR relaxation for droplets

For all samples studied (except the 24 ppm sample) a sharp phase transition is observed at low temperatures below which the NMR amplitudes are independent of temperature (see Fig. 4) as expected for the well-known phase separation

into Fermi liquid droplets.[64] The observed phase separation temperatures are in good agreement with the values calculated by Edwards and Balibar.[64] The rate of formation of the droplets is very slow (typically 2–10 h)[65] and great care must be taken to ensure that equilibrium is reached before measuring amplitudes and relaxation times near the phase separation. After phase separation, the relaxation times are observed to become temperature independent.[65,66] The observed relaxation times are consistent with a relaxation that occurs at the wall of degenerate Fermi liquid droplets. Huan *et al.*[65] showed that the relaxation time was given by $T_1 = (N_{\rm core}/N_{\rm wall})\tau_X$, where $N_{\rm core}$ and $N_{\rm wall}$ are the number of atoms in the core of the droplet and in the wall, respectively. τ_X is the intrinsic relaxation time at the wall due to the ^{3}He tunneling is given by $\tau_X = J_3/M_2$, where J_3 is the tunneling rate at the wall and M_2 is the NMR second moment. This estimate leads to values of $T_1 \sim 170$ s in good quantitative agreement with the observations (see Fig. 5).

V. CONCLUSION

Measurements of the nuclear spin-lattice relaxation times for very dilute ^{3}He concentrations have shown the existence of pronounced peaks in the relaxation times at the same temperatures as those for which anomalies are observed in torsional oscillator and shear modulus measurements of solid ^{4}He. Less well-defined variations are observed for the nuclear spin-spin relaxation times. The detailed temperature dependencies do not fit a model in which there is a well-defined phase transition to a supersolid or superfluid state where the critical fluctuations can induce dramatic changes in the relaxations times with critical exponents for the temperature dependence near the transition temperature. The observations are best described by the introduction of an additional relaxation process in series with the usual tunneling-relaxation process and caused by the response of the lattice to the motion of the lattice distortions around the tunneling impurity atoms. The characteristic parameters for this model, the tunneling rate, and the lattice excitation energy are remarkably close to those values deduced from measurements of the shear modulus. Further studies are needed at lower ^{3}He concentrations and lower magnetic fields to create a better separation between the phase separation temperature and the temperatures for which the NMR and other anomalies are observed.

ACKNOWLEDGMENTS

This research was carried out at the NHMFL High B/T Facility which is supported by NSF Grant DMR 0654118 and by the State of Florida. This project was supported in part by an award from the Collaborative Users Grant Program of the NHMFL. We gratefully acknowledge useful discussions with Sebastian Balibar, Moses Chan, Brian Cowan, Alan Dorsey, Izumi Iwasa, and Pradeep Kumar.

*Current address: École Polytechnique Fédérale de Lausanne, Lausanne, Switzerland.
†Current address: Georgia Institute of Technology, Atlanta, Ga, USA.
‡sullivan@phys.ufl.edu

[1] E. Kim and M. H. W. Chan, Nature (London) **427**, 225 (2004).
[2] E. Kim and M. H. W. Chan, Science **305**, 1941 (2004).
[3] A. J. Leggett, Phys. Rev. Lett. **25**, 1543 (1970).
[4] A. F. Andreev and I. M. Lifshitz, Sov. Phys. JETP **29**, 1107 (1969).
[5] E. Kim, J. S. Xia, J. T. West, X. Lin, A. C. Clark, and M. H. W. Chan, Phys. Rev. Lett. **100**, 065301 (2008).
[6] A. S. C. Rittner and J. D. Reppy, Phys. Rev. Lett. **97**, 165301 (2006).
[7] J. D. Reppy, Phys. Rev. Lett. **104**, 255301 (2010).
[8] E. J. Pratt, B. Hunt, V. Gadagkar, M. Yamashita, M. J. Graf, A. V. Balatsky, and J. C. Davis, Science **332**, 821 (2011).
[9] Y. Aoki, J. C. Graves, and H. Kojima, J. Low Temp. Phys. **150**, 252 (2008).
[10] P. Gumann, M. C. Keiderling, D. Ruffner, and H. Kojima, Phys. Rev. B **83**, 224519 (2011).
[11] P. Gumann, M. C. Keiderling, and H. Kojima, J. Low Temp. Phys. **168**, 162 (2012).
[12] J. M. Goodkind, Phys. Rev. Lett. **89**, 095301 (2002).
[13] P. C. Ho, I. P. Bindloss, and J. M. Goodkind, J. Low Temp. Phys. **109**, 409 (1997).
[14] X. Lin, A. Clark, and M. Chan, Nature (London) **449**, 1025 (2007).
[15] Y. Aoki, H. Kojima, and X. Lin, Low Temp. Phys. **34**, 329 (2008).
[16] S. Kwon, N. Mulders, and E. Kim, J. Low Temp. Phys. **158**, 590 (2010).
[17] J. Day and J. Beamish, Phys. Rev. Lett. **96**, 105304 (2006).
[18] M. W. Ray and R. B. Hallock, Phys. Rev. Lett. **100**, 235301 (2008).
[19] M. W. Ray and R. B. Hallock, Phys. Rev. B **79**, 224302 (2009).
[20] O. Syshchenko, J. Day, and J. Beamish, Phys. Rev. Lett. **104**, 195301 (2010).
[21] J. Day, O. Syshchenko, and J. Beamish, Phys. Rev. B **79**, 214524 (2009).
[22] O. Syshenko, J. Day, and J. Beamish, J. Phys.: Condens. Matter **21**, 164204 (2009).
[23] C.-D. Yoo and A. T. Dorsey, Phys. Rev. B **79**, 100504(R) (2009).
[24] M. Boninsegni, A. B. Kuklov, L. Pollet, N. V. Prokof'ev, B. V. Svistunov, and M. Troyer, Phys. Rev. Lett. **97**, 080401 (2006).
[25] P. W. Anderson, Science **324**, 631 (2009).
[26] B. Hunt, E. Pratt, V. Gadagkar, M. Yamashita, A. Balatsky, and J. C. Davis, Science **324**, 632 (2009).
[27] M. J. Graf, J. J. Su, H. P. Dahal, I. Grigorenko, and Z. Nussinov, J. Low Temp. Phys. **162**, 500 (2011).
[28] D. Y. Kim, H. Choi, W. Choi, S. Kwon, E. Kim, and H. C. Kim, Phys. Rev. B **83**, 052503 (2011).
[29] H. J. Maris, Phys. Rev. B **86**, 020502(R) (2012).
[30] J. R. Beamish, A. D. Fefferman, A. Haziot, X. Rojas, and S. Balibar, Phys. Rev. B **85**, 180501(R) (2012).
[31] D. Y. Kim and M. H. W. Chan, Phys. Rev. Lett. **109**, 155301 (2012).
[32] J. D. Eshelby, Solid State Phys. **3**, 79 (1956).
[33] A. Landesman, Phys. Lett. A **54**, 137 (1975).
[34] W. Huang, H. A. Goldberg, and R. A. Guyer, Phys. Rev. B **11**, 3374 (1975).
[35] I. Iwasa, Phys. Rev. B **81**, 104527 (2010).

[36]S. S. Kim, C. Huan, L. Yin, J. Xia, C. Candela, and N. S. Sullivan, J. Low Temp. Phys. **158**, 584 (2010).
[37]S. S. Kim, C. Huan, L. Yin, J. S. Xia, D. Candela, and N. S. Sullivan, Phys. Rev. Lett. **106**, 185303 (2011).
[38]C. Huan, S. S. Kim, L. Phelps, J. S. Xia, D. Candela, and N. S. Sullivan, J. Low Temp. Phys. **158**, 692 (2010).
[39]E. Grilly and R. L. Mills, Ann. Phys. (NY) **18**, 250 (1962).
[40]W. J. Mullin, Phys. Rev. Lett. **20**, 254 (1968).
[41]R. A. Guyer, R. C. Richardson, and L. I. Zane, Rev. Mod. Phys. **43**, 532 (1971).
[42]V. N. Grigoriev, B. N. Esel'son, V. A. Mikheev, V. A. Slusarev, M. A. Strzhemechny, and Y. E. Shulman, J. Low Temp. Phys. **13**, 65 (1973).
[43]J. Schratter, A. R. Allen, and M. G. Richards, J. Low Temp. Phys. **57**, 179 (1984).
[44]A. S. Greenberg, W. C. Thomlinson, and R. C. Richardson, J. Low Temp. Phys. **8**, 3 (1972).
[45]J. Day and J. Beamish, Nature (London) **450**, 853 (2007).
[46]A. Abragan and M. Goldman, *Nuclear Magnetism: Order and Disorder* (Clarendon, Oxford, 1982).
[47]N. V. Prokof'ev and G. V. Shlyapnikov, Zh. Eksp. Teor. Fiz. **93**, 2109 (1987).
[48]A. Landesman and J. M. Winter, *Proceedings Low Temperature Physics-LT-13* (Plenum, New York, 1974), pp. 73–78.
[49]A. Landesman, J. Low Temp. Phys. **30**, 117 (1978).
[50]N. Sullivan and A. Landesman, Phys. Rev. B **25**, 3396 (1982).
[51]V. A. Slyusarev, M. A. Strzhemechnyi, and I. A. Burakhovich, Fiz. Nizk. Temp. **3**, 1229 (1977).
[52]P. W. Anderson, Phys. Rev. **82**, 342 (1951).
[53]A. R. Allen, M. G. Richards, and J. Schratter, J. Low Temp. Phys. **47**, 289 (1982).
[54]I. Schuster, Y. Swirsky, E. J. Polturak, and S. G. Lipson, Europhys. Lett. **33**, 623 (1996).
[55]Y. Hirayoshi, T. Mizusaki, S. Maekawa, and A. Hideai, Phys. Lett. A **57**, 359 (1976).
[56]S. S. Kim, C. Huan, L. Yin, J. S. Xia, D. Candela, and N. S. Sullivan, J. Phys. Conf. Series **400**, 012031 (2012).
[57]R. Toda, P. Gumann, K. Kosaka, M. Kanemoto, W. Onoe, and Y. Sasaki, Phys. Rev. B **81**, 214515 (2010).
[58]R. Toda, W. Onoe, M. Kanemoto, T. Kakuda, Y. Tanaka, and Y. Sasaki, J. Low Temp. Phys. **162**, 476 (2011).
[59]M. A. Paalanen, D. J. Bishop, and H. W. Dail, Phys. Rev. Lett. **46**, 664 (1981).
[60]I. Iwasa, K. Araki, and H. Suzuki, J. Phys. Soc. Jpn. **46**, 1119 (1979).
[61]A. Haziot, A. D. Fefferman, J. R. Beamish, and S. Balibar, Phys. Rev. B **87**, 060509(R) (2013).
[62]S. Balibar (private communication).
[63]J. P. Franck, J. Gleeson, K. E. Kornelsen, J. R. Manuel, and K. A. McGreer, J. Low Temp. Phys. **58**, 153 (1985).
[64]D. O. Edwards and S. Balibar, Phys. Rev. B **39**, 4083 (1989).
[65]C. Huan, S. S. Kim, L. Yin, J. S. Xia, D. Candela, and N. S. Sullivan, J. Low Temp. Phys. **162**, 167 (2011).
[66]S. C. J. Kingsley, V. Maidonov, J. Saunders, and B. Cowan, J. Low Temp. Phys. **113**, 1017 (1998).